

Fluorescence Emission Study on Plastic Scintillator EJ-200 After Irradiation

Alberto Belloni^a, Sarah Eno^a, Yongbin Feng^a, Charles Hurlbut^b, Aaron Hunt^a, Geng-Yuan Jeng^a, Zachary Thomas^a, Yao Yao^a, Zishuo Yang^a

^a*Department of Physics, University of Maryland, College Park, MD 20740, USA*

^b*Eljen Technology, 1300 W. Broadway, Sweetwater, TX 79556, USA*

Abstract

Fluorescence emission yield versus wavelengths for plastic scintillator EJ-200 of various dopant concentrations is measured, before and after irradiation by ^{60}Co source for various doses and dose rates. Dose, dose rate, and temperature effects on dopants during irradiations are investigated.

Keywords: plastic scintillator, fluorescence, radiation damage, spectrophotometer

1. Introduction (to add more)

Organic plastic scintillators made of polystyrene (PS) or polyvinyltoluene (PVT) substrate and wavelength-shifting dopants have long been popular in detectors used in particle physics, nuclear physics, radiation safety, and health physics applications due to their high light output, low cost, fast response, and versatility of physical construction. Prolonged exposure of plastic scintillator to ionizing radiation, however, can result in damage such that absorption in the substrate increases and the transfer efficiency from initial excitation of the substrate to the dopants combined with a dopant's probability of radiative relaxation lessens. In this paper, we present fluorescence yield measurements before and after gamma irradiation of various doses and dose rates, for one type of plastic scintillator manufactured by Eljen Technology, EJ-200 (similar to BC-408 from Bicron) with different concentrations of the primary and secondary dopant. Dose rate effects are of interest because material-testing is typically done at much higher dose rates than which the scintillator will experience in use, due to reactor-time cost. Dose rate effects

may be responsible for the factor-of-three-larger light loss with integrated luminosity in the Compact Muon Solenoid (CMS) endcap hadron calorimeter (to cite) than expected based on high dose rate exposure using ^{60}Co sources (to cite).

The effect of dose and dose rate on radiation-induced absorption increase have been the subject of many investigations (to cite). The presence of oxygen plays an important role during and after irradiation (to cite). The studies show that the penetration depth of oxygen into the substrate depends on the dose rate: at lower dose rates, oxygen penetrates more deeply (to cite). Because of the importance of the interaction of oxygen with radicals produced from the substrate during irradiation, this can lead to dose rate effects. Two types of interactions occur in this process. The presence of oxygen increases the number of migration mechanisms for the radicals produced during irradiation. This allows the radicals that can create color centers which absorb light to migrate, find other radicals, and reform chemical bonds that do not create color centers. However, as discussed in (to cite Bross), Oxygen also interacts with the radicals produced during irradiation in a way that forms color centers.

Studies on the radiation damage effect on the light yield are fewer than those on the absorption. Several studies indicate that damage is to the substrate or the transfer of substrate's emission to dopants, rather than on the dopants themselves. Some studies have indicated that while oxygen plays a beneficial role in regards to annealing of induced absorption effects after irradiation, it plays a detrimental role in regards to light output (to cite).

In order to understand the relative role of destruction of the dopants versus damage to the substrate for modern plastic scintillators, we have studied the light output for plastic scintillator EJ-200 with various dopant concentrations, for different total doses and dose rates.

2. Sample and Irradiation

EJ-200 uses PVT as a substrate. It has a light output that is 60% of anthracene and a maximum-emission wavelength of 425 nm (blue). Eljen Technology prepared the samples with dimensions of 1x1x5 cm³. The samples were made with concentration of the primary and secondary dopants at 1.0 and 2.0 that of the nominal concentration (which has optimized light output before irradiation). 1P and 2P refer to nominal and double the nominal concentration of the primary, while 1X and 2X refer to nominal and double

the nominal concentration of the secondary. The samples for irradiation were wrapped in Tyvek sheets and were in contact with air. Using the LHC beamline irradiation facility (CASTOR) at CERN, one 1X and one 2X sample were irradiated at about 0.24 krad/hr for a total dose of 0.24 Mrad. (to add uncertainties) Using a ^{60}Co source at the National Institute of Standard and Technology (NIST), some 1P and 2P samples were irradiated at rates of 10 krad/hr and 429 krad/hr for a total dose of 3 Mrad, at about 23 °C ambient temperature. Using a ^{60}Co source at NASA, one 1P and one 2P sample were irradiated at 10 krad/hr for a total dose of 4 Mrad, at about 23 °C ambient temperature; Two samples that previously received 3 Mrad at 10 krad/hr at NIST were irradiated again at 10 krad/hr for an additional dose of 4 Mrad; Two 1X samples were irradiated at 80 krad/hr for 5.8 Mrad, at different temperatures 23 °C and -30 °C. Additional samples that were produced in the same batch were kept non-irradiated for calibration and comparison. Table 1 summarizes the samples irradiated in this study.

Table 1: Summary of irradiated EJ-200 samples. 1P and 2P refer to nominal and double the nominal concentration of the primary dopant, while 1X and 2X refer to nominal and double the nominal concentration of the secondary dopant.

Dopant concentration	Dose (Mrad)	Dose rate (krad/hr)
1P	3 \pm	10 \pm
2P	3 \pm	10 \pm
1P	3 \pm	429 \pm
2P	3 \pm	429 \pm
1P	4 \pm	10 \pm
2P	4 \pm	10 \pm
1P	7 \pm	10 \pm
2P	7 \pm	10 \pm
1X	0.24 \pm	0.24 \pm
2X	0.24 \pm	0.24 \pm
1X at 23 °C	6 \pm	80 \pm
1X at -30 °C	6 \pm	80 \pm

3. Instrumentation and Techniques

The fluorescence emission spectra were measured using a FluoroMax-Plus fluorescence spectrometer by Horiba Scientific. The spectrometer uses

a Xenon arc lamp as continuous light source. Light from the lamp is collected by a diamond-turned elliptical mirror and focused on the entrance slit of the excitation monochromator. The entrance and exit slits of the excitation monochromator are continuously adjustable, which controls the bandpass of the excitation beam. A toroidal mirror focuses the excitation beam onto the sample, while a small amount of the beam is split off by a beam-splitter to the reference silicon photodiode. Fluorescence emission produced by the sample is subsequently collected at ninety-degree angle with respect to the excitation beam. Similar to the excitation monochromator, the emission monochromator selects the bandpass of emission light that is sent to a Hamamatsu R928 photomultiplier tube (PMT). After correcting signals of the PMT and the photodiode according to their quantum efficiencies, the fluorescence emission signal is calculated as the ratio of the PMT's signal over the photodiode's signal. For each fluorescence spectrum measurement, a fixed excitation wavelength is used, and the emission intensity at a range of wavelengths is measured.

In order to study the effect of radiation damage on the primary and secondary dopants, three excitation wavelengths were chosen: 285 nm exciting PVT and the primary dopant, 350 nm exciting the secondary and primary dopants, and 400 nm exciting mostly the secondary dopant. The sample placement in the spectrometer adopts the front-surface configuration (shown in Figure 1), which gives the excitation beam a sixty-degree incident angle and maximizes fluorescence emission at the surface. This minimizes the effect of self absorption when measuring fluorescence yield after irradiation.

4. Measurements

After irradiations, the samples showed coloration which partially disappeared after time due to the annealing of the substrate. The samples were repeatedly measured after irradiation until no additional annealing was shown. Typical fluorescence spectra of EJ-200 is shown in Figure 2, after 3 Mrad at 10 krad/hr and after 3 Mrad at 429 krad/hr.

We calculate the light yield ratio (R) using the integrated area of the irradiated sample's spectrum with respect to the corresponding non-irradiated one.

Table 2 shows the ratio of light output excited at three different wavelengths for 1P (1P1X?) samples of different doses and dose rates.

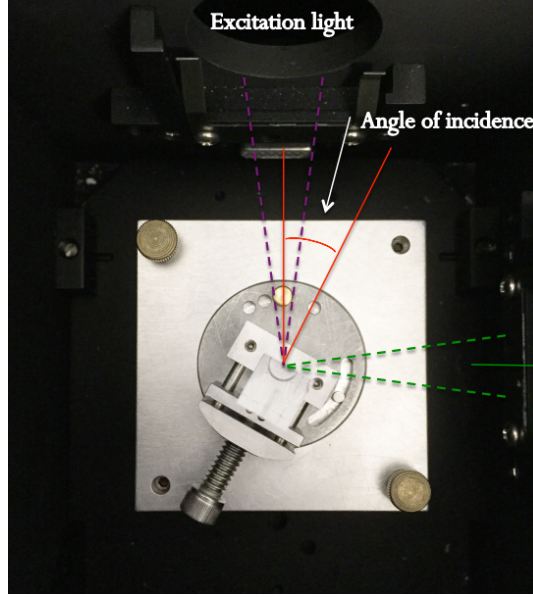


Figure 1: Front-surface configuration for fluorescence spectrum measurements.

Table 3 shows the ratio of light output excited at three different wavelengths for 1P (1P1X?) samples of different doses at dose rate 10 krad/hr.

Table 4 shows the ratio of light output excited at three different wavelengths for 1X (1P1X?) samples of same dose (5.8 Mrad) and dose rate (80 krad/hr), but at two different ambient temperatures (23 °C and -30 °C) during irradiation.

Table 2: Light output ratio after irradiations of different doses and dose rates.

Dose (Mrad)	Dose rate (krad/hr)	R at 285 nm	R at 350 nm	R at 400 nm
0.24±	0.24±	0.94±	0.94±	0.89±
3.0 ±	10 ±	0.95±	0.95±	0.92±
3.0 ±	430±	0.95±	0.92±	0.84±

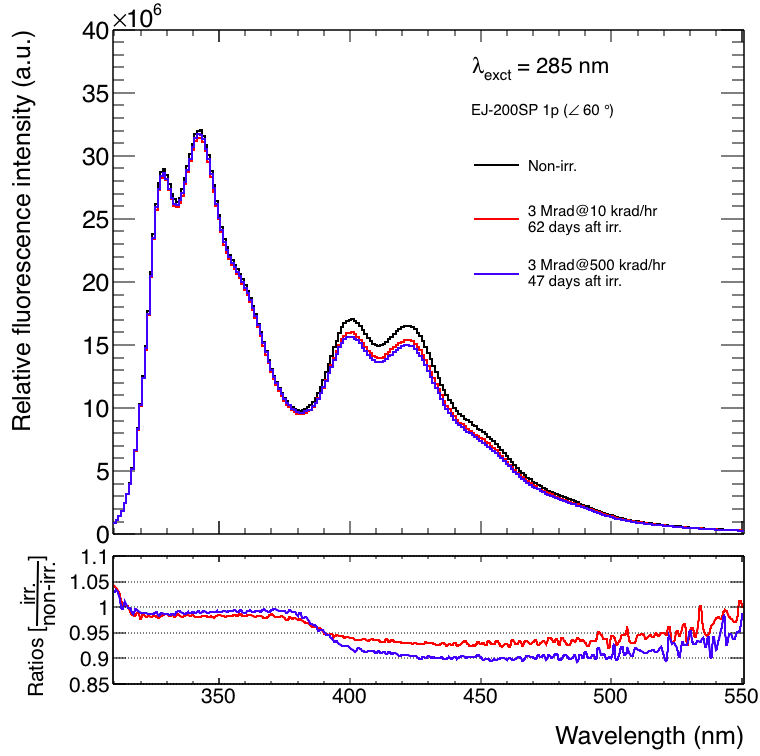


Figure 2: Fluorescence spectrum excited at 285 nm.

Table 3: Light output ratio after irradiations of different total doses at dose rate 10 krad/hr.

Dose (Mrad)	R at 285 nm	R at 350 nm	R at 400 nm
3.0 \pm	0.95 \pm	0.95 \pm	0.92 \pm
4.0 \pm	0.94 \pm	0.92 \pm	0.88 \pm
7.0 \pm	0.91 \pm	0.88 \pm	0.82 \pm

Table 4: Light output ratio after irradiations of the same dose and dose rate at 23 °C and -30 °C.

T (°C)	R at 285 nm	R at 350 nm	R at 400 nm
23 \pm	0.90 \pm	0.88 \pm	0.78 \pm
-30 \pm	0.91 \pm	0.84 \pm	0.70 \pm